

A simple technique for avoiding convergence problems in finite element simulations of crack nucleation and growth on cohesive interfaces

Y F Gao and A F Bower

Division of Engineering, Brown University, Providence, RI 02912, USA

Received 26 October 2003

Published 12 March 2004

Online at stacks.iop.org/MSMSE/12/453 (DOI: 10.1088/0965-0393/12/3/007)

Abstract

Numerical simulations of crack initiation which use a cohesive zone law to model a weak interface in the solid are often limited by the occurrence of an elastic snap-back instability. At the point of instability, quasi-static finite element computations are unable to converge to an equilibrium solution, which usually terminates the calculation and makes it impossible to follow the post-instability behaviour. In this paper, we show that such numerical difficulties can easily be avoided by introducing a small viscosity in the constitutive equations for the cohesive interface. Simple boundary value problems are used to develop guidelines for selecting appropriate values of viscosity in numerical simulations involving crack nucleation and growth. As a representative application, we model crack nucleation at the interface between an elastic thin film and an elastic–plastic substrate, which is subjected to contact loading.

1. Introduction

Cohesive interface models are often used in numerical simulations of void nucleation or fracture in materials subjected to mechanical or thermal loading. Examples include finite element simulations of void nucleation in metal-matrix composites [1], dynamic crack growth in brittle solids [2, 3] and crack initiation during indentation of a thin film on a ductile substrate [4], among many others. In all these computations, the cohesive law is used to model the behaviour of a weak interface in the solid, which separates when subjected to a sufficiently large stress. When the cohesive zone law is used to model the growth of a long pre-existing crack in the solid, the simulation generally proceeds without difficulty. Computations that use cohesive zones to model crack nucleation, however, often experience convergence difficulties at the point where the crack first nucleates. These problems are known to arise from an elastic snap-back instability, which occurs just after the stress reaches the peak strength of the interface. In an implicit finite element formulation (which uses Newton–Raphson iteration to solve the nonlinear equilibrium equations) one finds that the radius of convergence of the Newton–Raphson scheme reduces to zero at the point of instability. In an explicit scheme, the solution quickly diverges from the equilibrium path and leads to unphysical predictions.

Various approaches can be used to resolve these convergence problems: for example, one can prescribe the magnitude of the opening displacements at the incipient crack while leaving the remote loading as a variable; alternatively, general-purpose schemes such as the Riks method [5] may be used to follow the unstable branch of the solution during the snap-back. In general, these schemes require some effort to implement, and in history dependent problems (such as those involving plasticity or dislocation motion) it is not clear that following the unstable equilibrium solution necessarily leads to physically meaningful predictions.

In this paper, we show that the convergence difficulties can be avoided completely by introducing a small fictitious viscosity in the cohesive zone law that characterizes the interface. This modification is extremely simple to implement, requiring no more than two additional lines in a typical finite element code. We have tested this approach in several applications, involving both elastic and elastic–plastic materials, in both two and three dimensions, and have found that in all cases the computations can model unstable crack nucleation without difficulty. In addition, our tests show that although the additional viscosity makes the solution rate dependent, and may introduce additional energy dissipation into the computations, the solution will converge (for a sufficiently small time-step) for any nonzero value of viscosity. Consequently, in any given problem the viscosity can always be made small enough so that viscous energy dissipation is negligible during stable crack growth, in which case the viscosity has no effect on the solution. During unstable crack growth or crack nucleation, the viscous term in the cohesive law always dissipates energy, but the additional energy dissipation can easily be computed, and for sufficiently small values of viscosity will approach a value that depends on the (reversible) work of separation of the interface, the specimen geometry and properties, but is independent of viscosity. In problems involving unstable crack nucleation or growth, this additional dissipation can be regarded as approximately equivalent to the energy that would be radiated from the crack in elastic waves during the instability.

This is, of course, not the first time that energy dissipation has been incorporated in a cohesive zone model. Fracture is an inherently dissipative process, and various history dependent constitutive equations have been developed to model irreversibility in both brittle and ductile solids (e.g. [6–9]). In contrast to these models, our goal here is merely to regularize unstable behaviour during crack nucleation, rather than to model realistically any mechanism of fracture. We adopt the simplest possible form for the interface model, and then study the consequences of using our constitutive law in representative applications, both from the point of view of its effect on convergence of finite element simulations, and also to understand its effect on the conditions necessary to nucleate and propagate cracks on the weak interface.

The remainder of this paper is organized as follows. In the next section, we outline briefly how viscosity can be introduced into the constitutive equations for a cohesive interface, using the Xu–Needleman interfacial constitutive law as a representative example. We then solve a simple boundary value problem to illustrate the origin of the snap-back instability that occurs when this law is used to model crack initiation at a stressed interface. This model is used to demonstrate the influence of viscosity on both the behaviour of the interface, and on the convergence and accuracy of fully implicit finite element simulations that make use of the dissipative interface model. Finally, as a representative example, we use the modified interface law to model crack nucleation at the interface between a hard coating and a plastic substrate, when the solid is indented by a hard sphere.

2. Dissipative cohesive zone law

Cohesive zone laws are intended to model weak interfaces in a solid, which may separate when subjected to a sufficiently large stress. Consider a solid in which this weak interface occupies

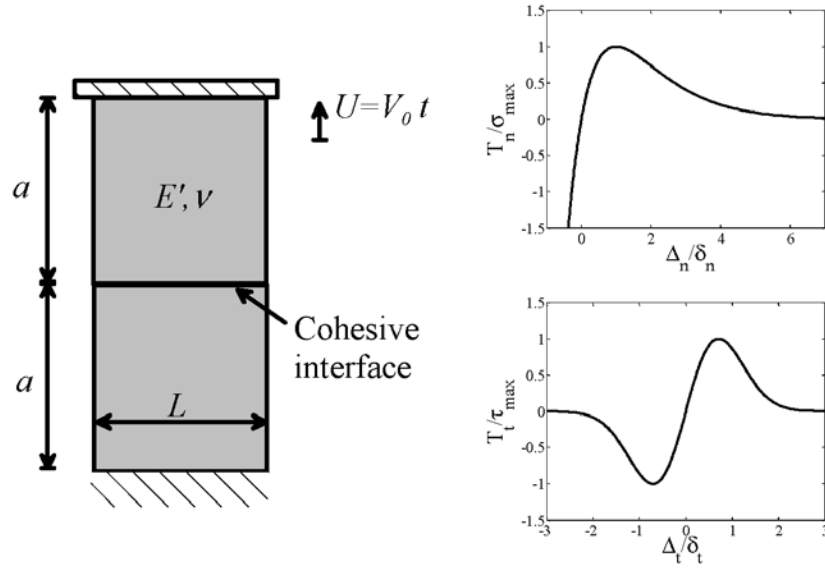


Figure 1. The simple boundary value problem used to test the influence of viscosity in the cohesive interface model. The graphs show the traction–displacement relations defined by equation (3).

a plane S . Introduce an arbitrary coordinate system (ξ, η) on S , and at each point define an orthonormal basis $\{\mathbf{n}, \mathbf{t}^{(1)}, \mathbf{t}^{(2)}\}$ where \mathbf{n} denotes the normal to S and $\mathbf{t}^{(\alpha)}$, where $\alpha = 1, 2$ denote two tangent vectors on S . Let $\mathbf{u}(\mathbf{x})$ denote the (infinitesimal) displacement field in the solid, which is continuous everywhere except on S , and let $\mathbf{u}^\pm(\mathbf{x}) = \lim_{\varepsilon \rightarrow 0} \mathbf{u}(\mathbf{x} \pm \varepsilon \mathbf{n})$ denote the limiting values of displacement on each side of the interface. The normal and tangential displacement discontinuity across S follows as $\Delta_n = (\mathbf{u}^+ - \mathbf{u}^-) \cdot \mathbf{n}$, $\Delta_{t\alpha} = (\mathbf{u}^+ - \mathbf{u}^-) \cdot \mathbf{t}^{(\alpha)}$. In addition, let $\boldsymbol{\sigma}$ denote the stress field in the solid, and let $T_n = \mathbf{n} \cdot \boldsymbol{\sigma} \cdot \mathbf{n}$, $T_{t\alpha} = \mathbf{n} \cdot \boldsymbol{\sigma} \cdot \mathbf{t}^{(\alpha)}$ denote the normal and tangential tractions acting on S . The cohesive interface law relates $(\Delta_n, \Delta_{t\alpha})$ and $(T_n, T_{t\alpha})$. For an ideal elastic interface, the relationship is defined by an elastic potential function ϕ such that

$$T_n = \frac{\partial \phi}{\partial \Delta_n} \quad T_{t\alpha} = \frac{\partial \phi}{\partial \Delta_{t\alpha}} \tag{1}$$

Various forms of ϕ have been used in numerical simulations. Here, we will use one developed by Xu and Needleman [2]

$$\begin{aligned} \phi(\Delta_n, \Delta_t) = & \phi_n + \phi_n \exp\left(-\frac{\Delta_n}{\delta_n}\right) \left\{ \left[1 - r + \frac{\Delta_n}{\delta_n} \right] \frac{1 - q}{r - 1} \right. \\ & \left. - \left[q + \left(\frac{r - q}{r - 1} \right) \frac{\Delta_n}{\delta_n} \right] \exp\left(-\frac{\Delta_t^2}{\delta_t^2}\right) \right\} \end{aligned} \tag{2}$$

where $\Delta_t = \sqrt{\Delta_{t1}^2 + \Delta_{t2}^2}$, and $\phi_n, \delta_n, \delta_t, q$, and r are constitutive parameters. The stress–displacement relations resulting from this potential are sketched in figure 1. Under normal loading the interface has a work of separation ϕ_n , and the normal traction reaches a maximum value $\sigma_{\max} = \phi_n / (\delta_n \exp(1))$ at an interface separation $\Delta_n = \delta_n$. Under purely shear loading, the interface has work of separation $q\phi_n$, and the tangential traction reaches a maximum value $\tau_{\max} = q\phi_n \sqrt{2} / (\delta_t \sqrt{\exp(1)})$ at $\Delta_t = \delta_t / \sqrt{2}$.

The objective of this paper is to investigate the effect of adding a small additional viscous dissipation to the interface model defined by equations (1) and (2). To this end, we write the traction–displacement relation for the interface as

$$\begin{aligned} T_n &= \sigma_{\max} \exp\left(1 - \frac{\Delta_n}{\delta_n}\right) \left\{ \frac{\Delta_n}{\delta_n} \exp\left(-\frac{\Delta_t^2}{\delta_t^2}\right) + \frac{1-q}{r-1} \left[1 - \exp\left(-\frac{\Delta_t^2}{\delta_t^2}\right)\right] \left[r - \frac{\Delta_n}{\delta_n}\right] \right\} \\ &\quad + \zeta_n \frac{d}{dt} \left(\frac{\Delta_n}{\delta_n}\right) \\ T_{t\alpha} &= 2\sigma_{\max} \left(\frac{\delta_n}{\delta_t}\right) \frac{\Delta_{t\alpha}}{\delta_t} \left\{ q + \left(\frac{r-q}{r-1}\right) \frac{\Delta_n}{\delta_n} \right\} \exp\left(1 - \frac{\Delta_n}{\delta_n}\right) \exp\left(-\frac{\Delta_t^2}{\delta_t^2}\right) + \zeta_t \frac{d}{dt} \left(\frac{\Delta_{t\alpha}}{\delta_t}\right) \end{aligned} \quad (3)$$

where ζ_n and ζ_t are viscosity-like parameters that govern viscous energy dissipation under normal and tangential loading, respectively. The viscosity is not intended to model any physical energy dissipation process, but is introduced to regularize instabilities that tend to occur when a crack first initiates on the weak plane. In the following, we explore the role of this regularization on numerical simulations of crack nucleation on weak interfaces.

3. Example boundary value problem

A simple example of a problem involving decohesion at a stressed interface is illustrated in figure 1. Two plane elastic strips with plane strain modulus E' , height a , and width L are connected by a weak interface on the plane $x_2 = 0$. The solid deforms in plane strain and is loaded (quasi-statically) by displacing the top boundary ($x_2 = a$) at constant vertical velocity V_0 , while holding the bottom boundary ($x_2 = -a$) fixed. The boundaries at $x_1 = \pm L/2$ are traction free. The interface is modelled using the cohesive zone law described in the preceding section: for simplicity we choose parameter values $q = 1$, $r = 0$. Our objective is to calculate the vertical stress $\sigma_{22} = \sigma$ in the solid, and the separation of the interface Δ , as a function of the displacement $U = V_0 t$ (where t denotes time) of the top interface.

We focus first on the solution with zero viscosity ($\zeta_n = 0$). A trivial calculation shows that the stress is related to the separation of the interface by

$$\frac{\sigma}{\sigma_{\max}} = \frac{\Delta}{\delta_n} \exp\left(1 - \frac{\Delta}{\delta_n}\right) \quad (4)$$

while the displacement of the top boundary is given by

$$\frac{E'U}{2a\sigma_{\max}} = \frac{\Delta}{\delta_n} \left\{ \Lambda + \exp\left(1 - \frac{\Delta}{\delta_n}\right) \right\} \quad (5)$$

where $\Lambda = E'\delta_n/(2a\sigma_{\max})$ is a dimensionless constant, which specifies the stiffness of the solid compared with that of the interface.

The resulting relationship between normalized stress σ/σ_{\max} and displacement $E'U/(2a\sigma_{\max})$ is shown in figure 2(a), for several values of Λ , while figure 2(b) shows the relationship between the interface separation $\Lambda\Delta/\delta_n$ and $E'U/(2a\sigma_{\max})$ (which is equal to $\Lambda U/\delta_n$). For $\Lambda > \exp(-1)$, one finds that the stress and interface separation are single-valued functions of the displacement of the boundary, implying that the interface separates smoothly. For $\Lambda < \exp(-1)$, the stress–displacement curve has an unstable branch. If the solid is loaded by progressively increasing the displacement of the top boundary, the interface will snap open, with a sudden jump in displacement, and a corresponding drop in stress. If the motion of the top boundary were subsequently reversed, the interface would remain open until the attractive forces on the opposing sides of the interface are sufficient to snap

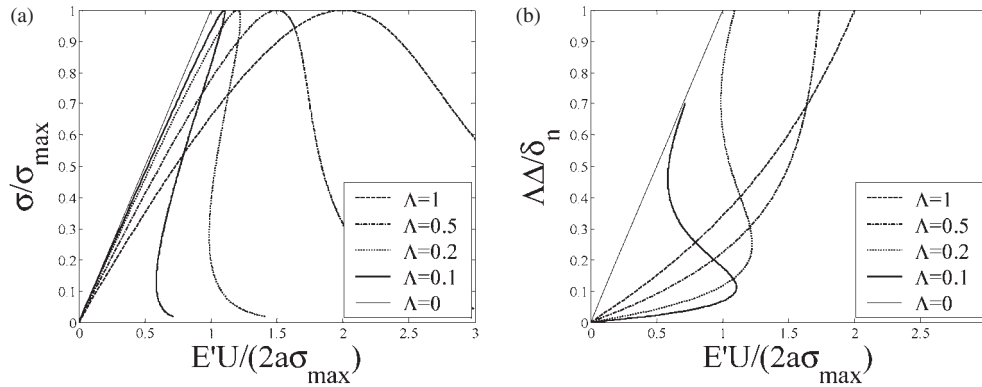


Figure 2. (a) Normal stress and (b) cohesive interface separation as a function of boundary displacement for several values of Λ .

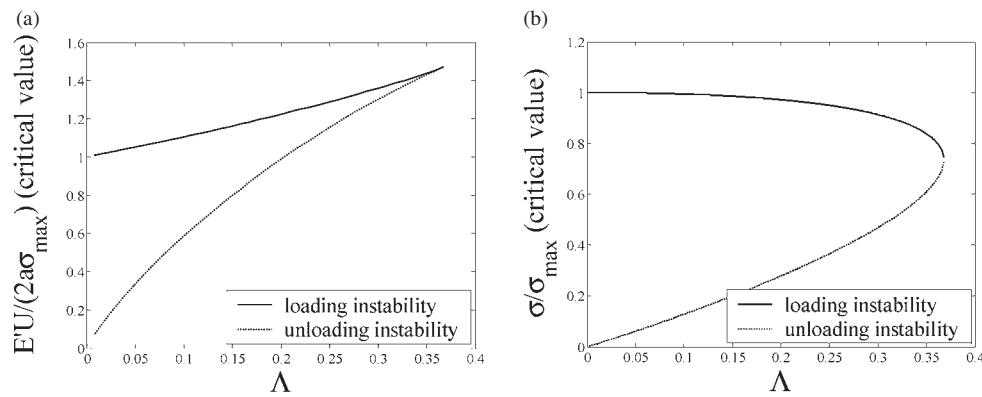


Figure 3. Critical boundary displacement (a) and critical stress (b) at the loading and unloading instability with varying Λ .

the interface closed. The critical boundary displacement and the critical stress at the point of instability during both loading and unloading are plotted as a function of Λ in figure 3. It is worth noting that the instability occurs neither when $\Delta = \delta_n$ nor when $\sigma = \sigma_{\max}$, implying that these criteria may not be reliable predictors of crack initiation in numerical simulations.

As a test case, we have set up this boundary value problem in the commercial finite element code ABAQUS [10], by implementing the cohesive zone as a user-element. The simulations used the default quasi-static time-stepping algorithm, with a maximum permissible time-step of order $\Delta t V_0/\delta_n = 0.1$, and without making use of the modified Riks algorithm implemented in ABAQUS. For values of $\Lambda > \exp(-1)$, the simulations proceed without difficulty, and correctly model the smooth separation of the interface. For $\Lambda < \exp(-1)$, however, the equilibrium iterations fail to converge just as the displacement approaches the point of instability, and the program terminates.

We next turn to investigate the influence of viscosity on the separation of the interface. Our main objective is to show that finite element computations have no difficulty converging when the viscous term is included in the constitutive response of the interface. To this end, we have plotted the stress and interface separation predicted by ABAQUS as a function of the normalized displacement of the top boundary $E'U/(2a\sigma_{\max})$ in figure 4. Since $U = V_0 t$,

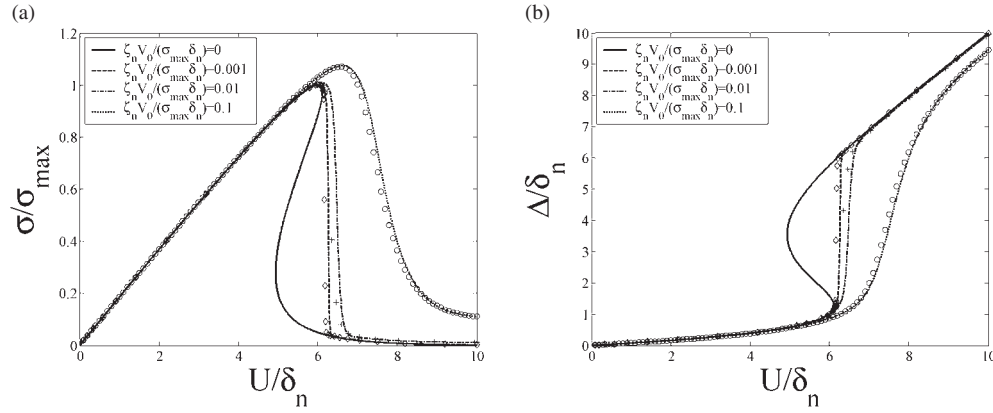


Figure 4. For several values of $\zeta_n V_0/(\sigma_{\max} \delta_n)$, (a) σ/σ_{\max} as a function of U/δ_n and (b) Δ/δ_n as a function of U/δ_n . In all the calculations, $\Lambda = \frac{1}{5}$.

the ordinate in this plot can be regarded also as a normalized measure of time. Results are shown for a dimensionless compliance $\Lambda = \frac{1}{5}$, and for several values of the dimensionless viscosity $\zeta_n V_0/(\sigma_{\max} \delta_n)$. The symbols in figure 4 show the results of quasi-static finite element computations, while the lines show the analytical solution. Evidently, the equilibrium iterations have no difficulty converging, although the time-step must be small enough to ensure that the change in displacement remains within the radius of convergence of the Newton–Raphson method. Numerical tests suggest that the appropriate time-step is approximately equal to the time-constant for stress relaxation after decohesion, which can be estimated as (using the limit for $\Lambda = 0$) as $t_0 \approx \zeta a/(E' \delta_n)$. For large values of normalized viscosity (or loading rate) $\zeta_n V_0/(\sigma_{\max} \delta_n) > 0.1$, the choice of time-step is governed by accuracy rather than stability: under these conditions one must take $\Delta t V_0/\delta_n < 0.1$.

Several general qualitative conclusions can be drawn from the simple boundary value problem considered here. First, we note that the condition for unstable interface separation $\Lambda < \exp(-1)$ can be written as $aL\sigma_{\max}^2/E' > L\phi_n/2$, which is the condition that the elastic strain energy released during debonding exceeds half the work of separation of the interface. This observation provides some insight into the origin of the convergence problems that occur in finite element models of crack nucleation. Convergence is guaranteed only if there exists a static equilibrium path that connects the states of the solid at the start and end of a time increment. Under fixed remote loading, the work done by the remote boundaries during debonding is positive or zero. Consequently, if the strain energy release rate during debonding exceeds the rate of work done against the cohesive zone tractions, a static equilibrium path cannot exist. Procedures such as the Riks method resolve this issue by providing a way for the remote boundaries to do negative work on the solid. Our approach here is to introduce a mechanism for dissipating the excess energy, thereby improving the likelihood that the numerical procedure will converge for a sufficiently small time-step.

This insight provides an approximate rule of thumb for estimating the critical combination of material properties that lead to unstable debonding in a more general boundary value problem. For example, suppose that we anticipate that the loading will nucleate a crack of length c on a bi-material interface that bonds solids with plane strain moduli E'_1, E'_2 . The crack will initiate when the stress on the interface reaches $T_n \approx \sigma_{\max}$. The change in elastic strain energy of the system during rapid crack initiation (with fixed remote boundary conditions) is approximately $\sigma_{\max}^2 \pi c^2/E'$ with $E' = E'_1 E'_2/(E'_1 + E'_2)$. This will exceed half the work of

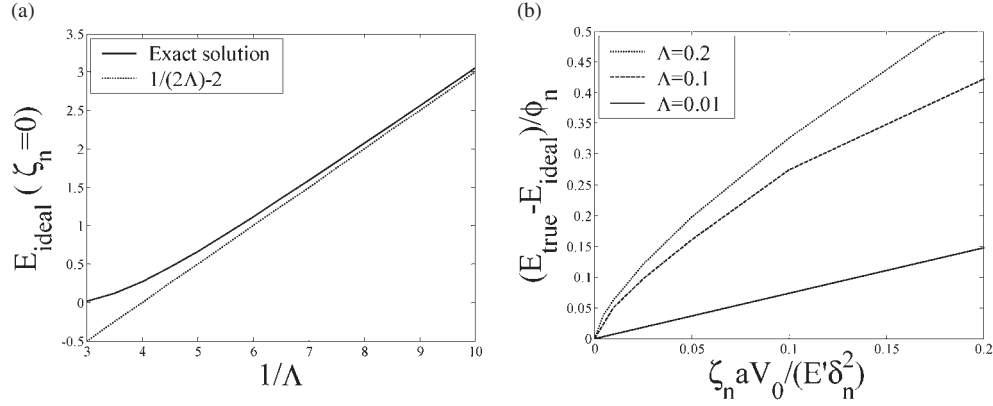


Figure 5. (a) Ideal energy dissipation as a function of $1/\Lambda$. (b) The ratio of actual and ideal energy dissipation as a function of viscosity.

separation if $\sigma_{\max}^2 \pi c^2 / E' > c \phi_n / 2$, suggesting that crack nucleation will be unstable if we select interface parameters σ_{\max} and δ_n so that $\delta_n / \sigma_{\max} < [2\pi / \exp(1)] c / E'$. A similar criterion can be developed for shear crack nucleation, and for other interfacial constitutive laws, but the details are left to the reader.

Since the viscosity in our interfacial constitutive law does not model any physical energy dissipation mechanism, it is of particular interest to ensure that the predictions of numerical simulations are insensitive to the value used for viscosity ζ . In a general quasi-static crack nucleation problem, the predictions will converge to a value that is independent of ζ as long as the interface separates (during the instability) much faster than any other characteristic time in the boundary value problem. A rough guide to selecting an appropriate value for ζ in the particular boundary value problem considered here can be obtained by estimating the time constant for stress relaxation (using the limit for $\Lambda = 0$) as $t_0 \approx \zeta a / (E' \delta_n)$, and ensuring that the displacement of the boundary during this time period is significantly less than the characteristic length δ_n in the separation law. This gives $\zeta a V_0 / (E' \delta_n^2) \ll 1$. To extend this to a more general boundary value problem, suppose that we expect to nucleate a crack with length $2c$ on a bi-material interface that bonds solids with plane strain moduli E'_1, E'_2 . The time constant for this configuration is approximately $t_0 \approx \pi c \zeta / E'$ with $E' = E'_1 E'_2 / (E'_1 + E'_2)$: as long as t_0 is significantly shorter than any other characteristic time in the boundary value problem, the solution should be independent of ζ . The same time constant can be used to estimate the time-step required to remain within the radius of convergence of the Newton–Raphson iterations; numerical tests suggest that $\Delta t < t_0$ will usually ensure convergence.

It should be apparent from the preceding discussion that the viscous term in the interface law will always lead to some energy dissipation during unstable crack nucleation. For sufficiently small ζ , the dissipated energy will converge to the difference between the elastic strain energy released during crack nucleation and the work done against the cohesive tractions during the instability (this limit is shown in figure 5(a) as a function of $1/\Lambda$; it is closely approximated by $\Delta E = 1/(2\Lambda) - 2$ for sufficiently small values of Λ). To illustrate the rate of convergence to this value with ζ , we have plotted the difference between the actual energy dissipated during time interval t_0 after debonding and the ideal energy dissipation for several values of $1/\Lambda$ in figure 5(b).

In the preceding discussion, we have focused on problems where cohesive zones are used to model crack nucleation. In many applications, cohesive zones are used to study the behaviour

of a long (and occasionally even semi-infinite) crack that propagates quasi-statically along a weak interface. Problems of this nature are less prone to convergence difficulties, since in most cases the crack propagation is inherently stable. Convergence problems will arise, however, if the crack growth is unstable: this will occur whenever the applied loading induces a crack tip energy release rate that exceeds the toughness of the cohesive interface. Again, under these conditions there is no static equilibrium path connecting the states of the solid at the start and end of a time-step, and convergence cannot be guaranteed. A trivial example is provided by the propagation of a slit crack of length $2c$ along a cohesive interface with toughness ϕ_n under constant remote stress σ . The crack starts to propagate when the crack tip energy release rate reaches $\pi\sigma^2c/E' = \phi_n$. When the crack reaches a length $2(c + \Delta c)$, the energy release rate $\pi\sigma^2(c + \Delta c)/E' > \phi_n$, so a static equilibrium solution does not exist.

The interfacial constitutive law proposed in equation (3) can be used to regularize problems of this nature, but it should be applied with caution. To illustrate the effect of the viscous term on the behaviour of a propagating crack, consider a planar, semi-infinite crack in an infinite elastic solid. At time $t = 0$, the crack tip lies at $x_1 = 0$, and a cohesive interface lies ahead of the crack. The solid is subjected to mode I loading so as to induce a far-field energy release rate $G^\infty > \phi_n$. For simplicity, we consider the limit $G^\infty \rightarrow \phi_n$, in which case the viscous term in (3) has a negligible influence on the crack opening displacements. Under these conditions, the crack opening displacements remain self-similar as the crack advances.

It is particularly instructive to estimate the energy dissipated due to the presence of the viscous term in the interfacial constitutive law. To this end, suppose that at time t , the crack has propagated a distance Δa and has instantaneous crack tip speed V_0 . Energy conservation gives

$$G^\infty = \phi_n + \frac{V_0\zeta}{\delta_n} \int_{-\infty}^{\Delta a} \left(\frac{d\Delta(r)}{dr} \right)^2 dr \quad (6)$$

where $\Delta(r)$ denotes the interface separation as a function of distance r behind the crack tip. The second term on the right-hand side of equation (6) represents the additional energy dissipation resulting from the viscosity of the interface. It is not possible to calculate a closed-form expression for $\Delta(r)$ for the interface law specified by equation (3), but a rough quantitative estimate for the viscous energy dissipation can be obtained by approximating $\Delta(r)$ using the opening displacements for a Dugdale–Barenblatt crack with peak stress σ_{\max} and work of separation ϕ_n . This leads to

$$G^\infty = \phi_n + \frac{V_0\zeta}{\delta_n} \frac{\phi_n}{E'} \frac{8}{\pi} I \left(\frac{\Delta a}{b} \right) \quad (7)$$

where

$$I(x) = x \{ \coth^{-1}(\sqrt{1+x}) \}^2 + 2\sqrt{1+x} \coth^{-1} \sqrt{1+x} + \ln(x) \quad (8)$$

and $b = \pi E' \phi_n / (8\sigma_{\max}^2)$ is the approximate size of the crack tip cohesive zone, and where we have assumed $\Delta a > b$.

Several features of equation (7) are worthy of comment. In a practical application where the viscous interface law is used to model a brief period of unstable crack growth, the viscosity should be selected so that predictions are insensitive to the value of ζ . This is likely to be the case if the duration of unstable crack growth is much shorter than any relevant characteristic timescale in the problem. Equation (7) can be used to estimate the crack tip speed, and so provides a way to select an appropriate value for ζ . Disconcertingly, however, we find that the predicted crack tip speed decays logarithmically with the total crack extension Δa . This is not a serious limitation, since in actual computations Δa remains bounded, and as long as

the crack tip speed is large enough with the greatest expected value of Δa , the results should be insensitive to viscosity.

The dependence of viscous dissipation on crack length in equation (7) can also be avoided by using a more complex constitutive law for the interface. The dependence arises because the viscous term contributes to the traction acting on the crack faces even when the crack faces are a large distance apart. To avoid this, equation (3) may be replaced with a more complex relationship in which the viscosity varies with opening displacement. For example, one could set

$$\begin{aligned}
 T_n &= \sigma_{\max} \exp\left(1 - \frac{\Delta_n}{\delta_n}\right) \left\{ \frac{\Delta_n}{\delta_n} \exp\left(-\frac{\Delta_t^2}{\delta_t^2}\right) + \frac{1-q}{r-1} \left[1 - \exp\left(-\frac{\Delta_t^2}{\delta_t^2}\right)\right] \left[r - \frac{\Delta_n}{\delta_n}\right] \right\} \\
 &\quad \times \left(1 + \frac{\zeta_n}{\sigma_{\max}} \frac{d}{dt} \left(\frac{\Delta_n}{\delta_n}\right)\right) \\
 T_{t\alpha} &= 2\sigma_{\max} \left(\frac{\delta_n}{\delta_t}\right) \frac{\Delta_{t\alpha}}{\delta_t} \left\{ q + \left(\frac{r-q}{r-1}\right) \frac{\Delta_n}{\delta_n} \right\} \exp\left(1 - \frac{\Delta_n}{\delta_n}\right) \exp\left(-\frac{\Delta_t^2}{\delta_t^2}\right) \\
 &\quad \times \left(1 + \frac{\zeta_t}{\sigma_{\max}} \frac{d}{dt} \left(\frac{\Delta_{t\alpha}}{\delta_t}\right)\right)
 \end{aligned} \tag{9}$$

While these equations are somewhat more cumbersome to implement, numerical tests suggest that their effect on the accuracy and convergence of finite element calculations are indistinguishable from those of equation (3).

4. Application to interface crack initiation during indentation of a thin film on a substrate

Finally, as a representative practical application, we have modelled crack initiation at the interface between a hard elastic coating on an elastic–plastic substrate as a result of indentation by a rigid spherical indenter. Our objective is to show that the interface viscosity can successfully overcome convergence problems reported by Abdul-Baqi and Van der Giessen [4] when modelling this problem using the finite element method. The boundary value problem is illustrated in figure 7. We consider an elastic coating, with thickness w , Young's modulus E_c and Poisson's ratio ν_c , which is bonded to the surface of a semi-infinite substrate. The substrate is an elastic–perfectly plastic solid, with Young's modulus E_s , Poisson's ratio ν_s , and yield stress σ_Y . The interface between the coating and substrate is modelled using the cohesive zone defined in equation (3). The coating is indented by a rigid, frictionless spherical indenter with radius R . The indenter penetrates the surface with constant velocity V_0 and at time t reaches an indentation depth h . On reaching a penetration depth $h_{\max} = w/2$, the indenter is withdrawn at speed V_0 . The finite element program ABAQUS was used to compute the stress and displacement field in the solid, and hence to deduce the force F applied to the indenter. Specific parameter values used in our simulation are listed in the caption to figure 6. Abdul-Baqi and Van der Giessen [4] note that parameters q and r in the constitutive law defined by equation (2) must be chosen with care for any application where the interface is subjected to compressive loading: with an inappropriate choice the interface may lose shear strength under large compressive load. We have used $q = r = 0.5$ in the computations reported here. The estimates outlined in the preceding section suggest that $\zeta_n V_0 / (\sigma_{\max} \delta_n) = 0.00125$ is an appropriate choice of normalized viscosity for this simulation, and indicate that the time-step should be reduced to $\Delta t \approx 10^{-5}$ to ensure convergence during debonding. The automatic time-stepping procedure in ABAQUS selects a time-step very close to this value.

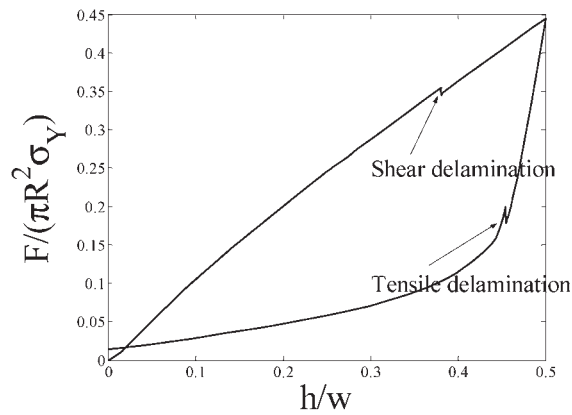


Figure 6. Load–displacement curve with $E_s/\sigma_Y = 400$, $E_c = E_s$, $\nu_c = \nu_s = 0.3$, $R/w = 10$, $\sigma_{\max}/\sigma_Y = 0.3$, $\delta_n = \delta_t = 0.002w$, $q = r = 0.5$, and $\zeta_n V_0/(\sigma_{\max}\delta_n) = 0.00125$.

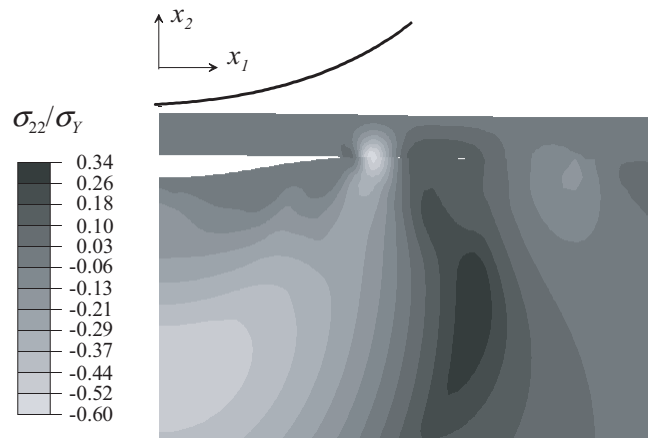


Figure 7. The final configuration and the distribution of vertical stress (normalized by yield stress σ_Y) of the coating system after complete unloading.

Figure 6 shows the dimensionless indentation force $F/(\pi R^2 \sigma_Y)$ as a function of the indentation depth h/w . Two discontinuities can be seen in the load–displacement curve: the discontinuity during loading occurs due to the unstable nucleation of a shear crack at position $r/w \sim 5$ on the interface. The second discontinuity in figure 6 corresponds to the nucleation of a tensile crack at position $r = 0$ under the contact, driven by tensile residual stresses that develop during unloading. The final configuration of the solid, together with the residual stress distribution is shown in figure 7. A large region of delamination is evident.

5. Conclusions

We have found that convergence problems that occur in finite element simulations of crack nucleation on a cohesive interface can be avoided by including a small viscous term in the constitutive equations for the interface. Including this term provides a mechanism for dissipating strain energy during unstable debonding, and therefore ensures that a quasi-static

equilibrium path exists connecting the state of the solid before and after the instability. By means of simple boundary value problems, we have explored the influence of the viscosity on convergence of numerical simulations involving crack nucleation, and also on the energetics of crack nucleation and growth. As a representative application, we have modelled crack initiation at the interface between a hard elastic coating on an elastic–plastic substrate as a result of indentation by a rigid spherical indenter. With the viscous interface model, we see no signs of the convergence problems reported by Abdul-Baqi and Van der Giessen [4] when modelling this problem.

Acknowledgments

This work was supported by the Brown/General Motors Collaborative Research Lab at Brown University. The authors are grateful to Bill Curtin and Alan Needleman for helpful discussions.

References

- [1] Povirk G L, Needleman A and Nutt S R 1991 An analysis of the effect of residual stresses on deformation and damage mechanisms in Al-SiC composites *Mater. Sci. Eng. A* **132** 31–8
- [2] Xu X P and Needleman A 1994 Numerical simulations of fast crack growth in brittle solids *J. Mech. Phys. Solids* **42** 1397–434
- [3] Miller O, Freund L B and Needleman A 1999 Energy dissipation in dynamic fracture of brittle materials *Modelling Simul. Mater. Sci. Eng.* **7** 573–86
- [4] Abdul-Baqi A and Van der Giessen E 2001 Delamination of a strong film from a ductile substrate during indentation unloading *J. Mater. Res.* **16** 1396–407
- [5] Crisfield M A 1981 A fast incremental/iteration solution procedure that handles ‘Snap-Through’ *Comput. Struct.* **13** 55–62
- [6] Roe K L and Siegmund T 2003 An irreversible cohesive zone model for interface fatigue crack growth simulation *Eng. Fract. Mech.* **70** 209–32
- [7] Tjssens M G A, Sluys B L J and Van der Giessen E 2000 Numerical simulation of quasi-brittle fracture using damaging cohesive surfaces *Eur. J. Mech. A/Solids* **19** 761–79
- [8] Blackman B R K, Hadavinia H, Kinloch A J and Williams J G 2003 The use of a cohesive zone model to study the fracture of fiber composites and adhesively-bonded joints *Int. J. Fract.* **119** 25–46
- [9] Landis C M, Pardo T and Hutchinson J W 2000 Crack velocity dependent toughness in rate dependent materials *Mech. Mater.* **32** 663–78
- [10] *ABAQUS 2002 V6.3 User’s Manual* (Pawtucket, Rhode Island, USA: ABAQUS Inc.)